

# Early Termination of Low-Density Parity-Check Codes for Continuous-Variable Quantum Key Distribution

Kadir Gümüş, João dos Reis Frazão, Vincent van Vliet, Menno van den Hout, Aaron Albores-Mejia, Thomas Bradley, and Chigo Okonkwo

<sup>(1)</sup> High-Capacity Optical Transmission Laboratory, Electro-Optical Communications Group, Eindhoven University of Technology, Eindhoven, The Netherlands, [k.gumus@tue.nl](mailto:k.gumus@tue.nl)

**Abstract** We analyse the impact of log a-posteriori early termination on the decoding throughput of reconciliation for continuous-variable quantum key distribution. Increases in decoded secret key rate throughput of up to 182% are reported in both simulations and experiments. © 2025 The Author(s)

## Introduction

Continuous-variable quantum key distribution (CV-QKD)<sup>[1]</sup> has garnered attention in recent years for the implementation of quantum secure key sharing using standard telecommunication components<sup>[2]</sup>. CV-QKD technology has significantly matured, and commercial products have become available<sup>[3]</sup>. However, the main bottleneck regarding the real-time implementation of CV-QKD systems is error correction, which limits the achievable key rates<sup>[4]</sup>.

Due to the quantum channel's low signal-to-noise ratio (SNR), complex error correction codes are required during reconciliation to ensure that the shared keys are identical between Alice and Bob. Although many experimental works on CV-QKD with high data rates exist<sup>[5]–[7]</sup>, the error correction is almost always done offline. Large clusters of A100 GPUs have been used for real-time error correction<sup>[8]</sup>, though this is expensive and impractical. Thus, the key rates reported are not achievable in practical systems. A popular class of error correction codes for CV-QKD are low-density parity check (LDPC) codes<sup>[9],[10]</sup>. These codes are decoded using belief propagation (BP), an iterative algorithm, where the number of iterations required for the decoding directly correlates to the speed of the decoding. Hence, lowering the number of decoding iterations allows for higher secret key rate (SKR) throughputs. High-speed implementations for CV-QKD do exist, however, these works either implement min-sum decoding<sup>[11]</sup>, which is not suitable for CV-QKD because of the significant loss of performance<sup>[12]</sup>, or focus on high-rate codes<sup>[13]</sup>.

In this paper, we investigate using early termination (ET) based on log a-posteriori probabilities for the high frame error rate (FER) regime for low-rate codes. We show that a simple ET algorithm can decrease the number of decoding iterations, increasing the SKR throughput by up to 182%. We validate these results using experimental data and show that decoded key rates almost triple.

## Early Termination

The BP algorithm used for LDPC decoding is an iterative algorithm that involves message passing along a bipartite graph, which is defined by the parity check matrix  $\mathbf{H}$ . Every iteration, the belief of

each bit is updated until the decoder has reached the maximum number of iterations  $D_{max}$ . For the low-rate LDPC codes used for CV-QKD,  $D_{max}$  is in the range of 200-500<sup>[5],[9]</sup>. One way to reduce the number of iterations is to use ET.

A popular method of ET is based on the calculation of the syndrome of the codeword estimate  $\hat{\mathbf{c}}$ , which has to be equal to 0, i.e.,  $\hat{\mathbf{c}}\mathbf{H} = \mathbf{0}$ <sup>[9]</sup>. In this case, the decoder has converged to a valid codeword, and thus, the decoder output will not change. This method works well when the FER is low. However, for the high FER regime, using the parity check equation (PCE) ET will often allow the decoding to continue until  $D_{max}$  has been reached, as the decoder does not converge.

In the high FER regime, we can use an ET method based on the log a-posteriori probabilities of the bits after each iteration<sup>[14]</sup>, which is referred to as variable node reliability early termination (VNR-ET). Let  $l_{out,i}^{(k)}$  be the log a-posteriori probability of bit  $i$  after  $k$  iterations. For each iteration, we calculate  $q^{(k)} = \sum_{i \in \mathcal{V}} l_{out,i}^{(k)}$ , where  $\mathcal{V}$  denotes

the set of variable nodes with degree higher than 1. Most variable nodes in low-rate LDPC codes are of degree 1, and these do not have to be considered when calculating  $q^{(k)}$ . For most correctly decoded codewords  $q^{(k)}$  increases monotonically, i.e.,  $q^{(k)} > q^{(k-1)}$ . With VNR-ET, we stop decoding if at any point  $q^{(k)} < q^{(k-1)}$ . Compared to the calculations of the  $\tanh$  and  $\operatorname{atanh}$  functions, this step adds a negligible amount of complexity<sup>[14]</sup>.

## Secret Key Rate

The SKR of a CV-QKD system is often expressed in bits/pulse and is given by<sup>[9]</sup>:

$$\text{SKR} = (1 - \text{FER})(\beta I_{AB} - \chi_{BE} - \Delta_n), \quad (1)$$

where  $I_{AB}$  is the mutual information between Alice and Bob,  $\chi_{BE}$  is the Holevo information, and  $\Delta_n$  is the finite-size penalty of the privacy amplification block size and depends on  $N_{privacy}$ <sup>[9]</sup>. The reconciliation efficiency  $\beta$  indicates how close the error correction is to the capacity and is defined as  $R/I_{AB}$ , where  $R$  is the rate of the code. There is a trade-off between  $\beta$  and FER, so the highest  $\beta$  will not always result in the highest SKR<sup>[15]</sup>. The

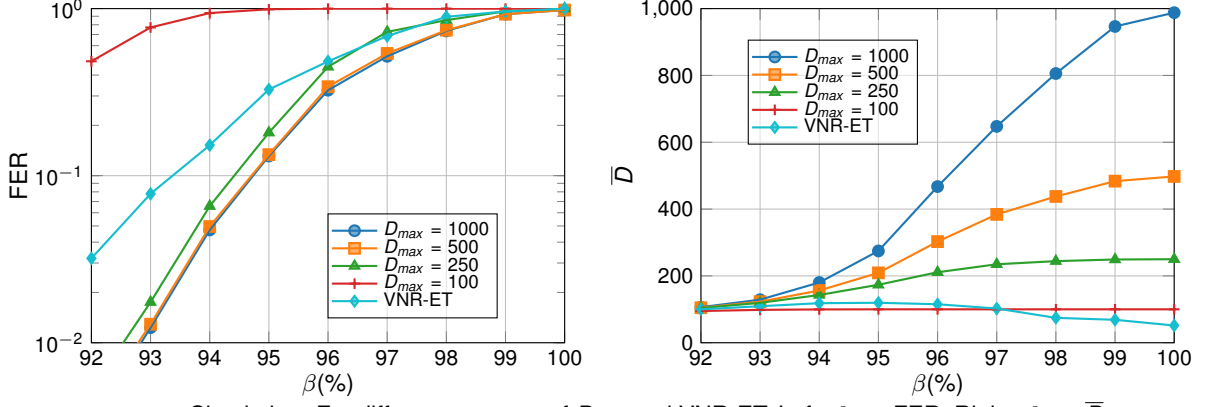


Fig. 1: Simulation: For different amounts of  $D_{max}$  and VNR-ET. Left:  $\beta$  vs. FER, Right:  $\beta$  vs.  $\bar{D}$ .

SKR throughput in bits/s is  $f_{rep}SKR$ , where  $f_{rep}$  is the pulse rate of the system.

The key rate related to the practical implementation of a CV-QKD system depends on the throughput of the error correction, which is smaller than SKR throughput in state-of-the-art works<sup>[4],[7]</sup>. The throughput  $K$  of an LDPC decoder in bits/t, where  $t$  is the latency per iteration, can be expressed as:

$$K = \frac{N}{\bar{D}}R(1 - FER), \quad (2)$$

where  $N$  is the blocklength of the code and  $\bar{D}$  is the average number of decoding iterations. The latency  $t$  is hardware-dependent and is not relevant for this analysis.

By substituting Eq. (2) into Eq. (1), the decoded SKR throughput in bits/t can be written as:

$$SKR_{dec} = \frac{N}{\bar{D}\mu}(1 - FER)(\beta I_{AB} - \chi_{BE} - \Delta_n). \quad (3)$$

where  $\mu = 1$  if homodyne detection is used, and  $\mu = 2$  if heterodyne detection is used. For the rest of the paper, heterodyne detection is assumed.

## Simulations

For the simulations in this section, we use a  $R = \frac{1}{50}$  type-based protograph (TBP) LDPC code<sup>[10]</sup> with blocklength  $N = 10^6$ . We have simulated for four different amounts of maximum decoding iterations

$D_{max} = \{100, 250, 500, 1000\}$  and for when using VNR-ET. In the case of VNR-ET, the  $D_{max}$  is unbounded, although during the simulations  $D$  never exceeded 300. In all cases, we use PCE-ET. For the CV-QKD system we assume the following variables: Gaussian modulation with modulation variance  $V_A$  chosen such that  $I_{AB} = \frac{R}{\beta}$ , heterodyne detection, quantum efficiency  $\eta = 0.4$ , electronic noise  $\nu_{el} = 0.01$ , excess noise on Bob  $\xi_{Bob} = 0.001$ , transmission distance  $d = 80$  km over an optical fibre with loss  $\alpha = 0.2$  dB/km, and privacy amplification blocklength  $N_{privacy} = 10^8$ .

In Fig. 1, we show FER (left) and  $\bar{D}$  (right) against the reconciliation efficiency  $\beta$ . The FER curve is the same for when  $D_{max} = 500$  and when  $D_{max} = 1000$ , indicating that more than 500 decoding iterations is unnecessary for this particular code. For  $D_{max} = 250$  the decrease in FER compared to  $D_{max} = 500$  is manageable; however, when we set  $D_{max}$  to 100, the performance decrease is very significant. In general, we found that when  $D_{max} < 250$ , the reduction in FER performance is too substantial to justify the decrease in  $D_{max}$ . For VNR-ET, we also get a penalty in FER, as we sometimes stop decoding a codeword which would have eventually converged. The average number of iterations when using VNR-ET is much lower when  $\beta$  is high, as the FER is high as well. When  $\beta$  decreases, the FER decreases; hence,

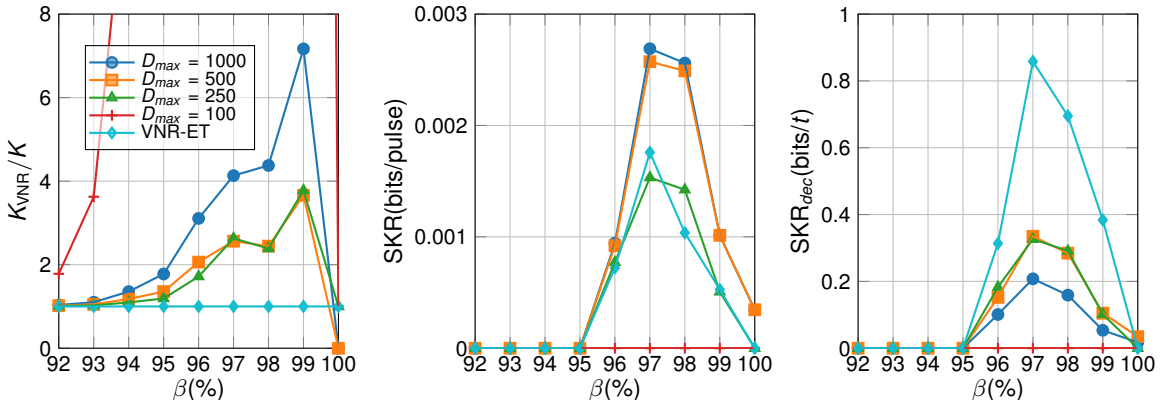


Fig. 2: Simulation: For different  $D_{max}$ , and for VNR-ET. Right:  $\beta$  vs.  $K_{VNR-ET}/K$ , Middle: SKR vs.  $\beta$ , Left:  $SKR_{dec}$  vs.  $\beta$ .

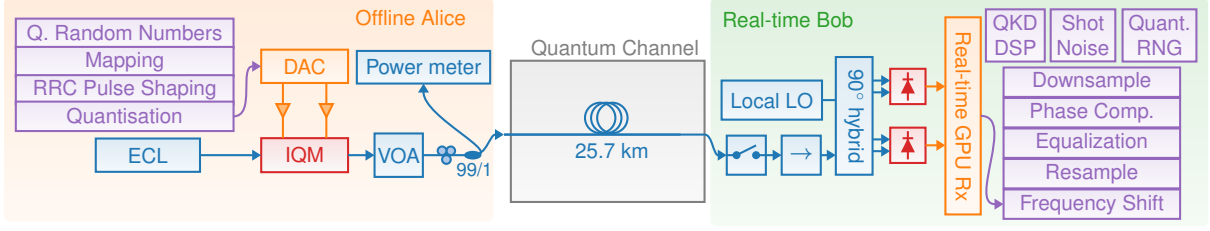


Fig. 3: Experimental set-up of CV-QKD over a 25.7 km fibre, with offline Alice and real-time GPU-based Bob

the number of codewords at which VNR-ET would have an effect decreases as well. As a result, for lower  $\beta$ ,  $\bar{D}$  is similar when using VNR-ET or not.

In Fig. 2 (left), we compare the ratio of  $K$  to  $K_{VNR-ET}$ , which is the throughput in the case of VNR-ET. As is shown,  $K_{VNR-ET}$  is always larger, despite the higher FER, except at  $\beta = 100\%$ . Here, the FER for VNR-ET is 1, while for  $D_{max} \geq 500$ , the FER is very close to 1 instead. Otherwise, as  $\beta$  increases, the throughput for VNR-ET increases.

In Fig. 2 (middle) and (right), we compare both SKR and  $SKR_{dec}$ , respectively, for the CV-QKD system previously described. The SKR for VNR-ET is smaller than for  $D_{max} \geq 500$ , but similar to  $D_{max} = 250$ . However, for  $SKR_{dec}$ , the throughput for VNR-ET outperforms the other curves, with a gain in  $SKR_{dec}$  of 182%. This gain depends on the optimal reconciliation efficiency  $\beta_{opt}$  of the CV-QKD system, as is shown in the next section.

### Experimental Results

Figure 3 shows our practical CV-QKD implementation. The offline transmitter (Alice) uses an external cavity laser (ECL) with a linewidth  $< 100$  kHz, IQ optical modulation for probabilistically shaped 256-QAM signals, and a 250 Mbaud symbol rate with 50% pilot symbols. Alice's average  $V_A$  was between 7 to 8 SNUs.

On Bob's side, a receiver operates in calibration and quantum signal reception mode by using an optical switch. Key system capabilities include an ECL as a local oscillator (LO) into an optical hybrid, digitisation at 2 GS/s, and real-time digital signal processing (DSP) for calibration and quantum signal analysis. DSP includes frequency-offset

compensation, filtering, equalisation, pilot-based phase recovery<sup>[16]</sup>, and parameter estimation.

Bob follows the trusted noise assumption, and all losses due to coupling and the optical isolator are considered in the quantum efficiency, resulting in a decrease in  $\eta$  from 67% to 40%. The average  $\xi_{Bob}$  is 0.0056 SNU, and we have a clearance of 10 dB. An isolator between the optical switch and the hybrid prevents back reflections from the local LO. Real-time post-processing on a GPU evaluates security via excess noise and SKR analyses.

For the error correction, we use an  $R = \frac{1}{5}$  expanded TBP-LDPC code punctured to the appropriate rate with  $N = 10^5$ . For each capture  $\beta$  was optimised to maximise SKR. Figure 4 shows the SKR for 32 different captures, comparing VNR-ET to only PCE-ET with  $D_{max} = 250$ . The captures have been sorted according to  $\beta_{opt}$  for VNR-ET. This fluctuates over the captures as the excess noise of the system fluctuates as well. The gains are small ( $< 10\%$ ) for cases where  $\beta_{opt} \leq 93\%$ . However, when  $\beta_{opt} = 97\%$ ,  $SKR_{dec}$  is almost tripled.  $SKR_{dec}$  decreases as  $\beta_{opt}$  increases, as these are the captures where  $I_{AB}$  and  $\chi_{BE}$  are closer to each other. VNR-ET would therefore offer a bigger improvement for systems which have to operate at high  $\beta$ , which would correspond more to CV-QKD systems with lower-grade components.

### Conclusion

In this work, we have shown how applying VNR-ET during decoding increases SKR throughputs because of the higher throughput of the decoder. We have demonstrated increases in  $SKR_{dec}$  of up to 182% in both simulations and experiments.

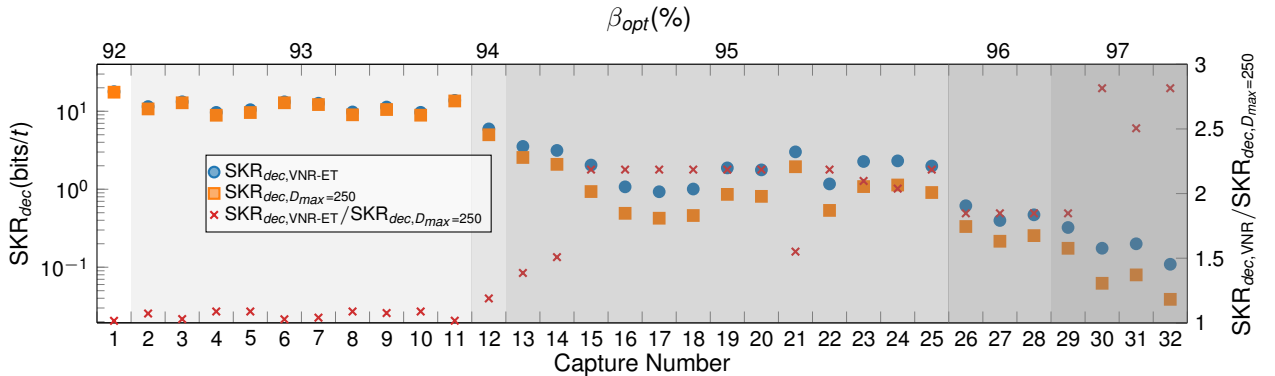


Fig. 4: Experiment: The  $SKR_{dec}$  for different CV-QKD captures comparing  $D_{max} = 250$  to VNR-ET. For error correction, an expanded TBP-LDPC code with  $R = \frac{1}{5}$  punctured to the appropriate rate is used. The captures are sorted according to at which  $\beta$   $SKR_{dec}$  was maximised for VNR-ET. Darker backgrounds correspond to higher  $\beta_{opt}$ .

## Acknowledgements

This work was supported by the PhotonDelta GrowthFunds Programme on Photonics and by the Dutch Ministry of Economic Affairs (EZ), as part of the Quantum Delta NL KAT-2 programme on Quantum Communications. This work also acknowledges the support of the European Union via the Marie Curie Doctoral Network QuNEST (Grant Agreement: 101120422) and the EIC Transition Grant project PAQAAL (under Grant Agreement 101213884)

## References

- [1] F. Grosshans, G. Van Assche, J. Wenger, R. Brouri, N. J. Cerf, and P. Grangier, "Quantum key distribution using Gaussian-modulated coherent states", *Nature*, vol. 421, no. 6920, pp. 238–241, 2003.
- [2] F. Laudenbach, C. Pacher, C.-H. F. Fung, *et al.*, "Continuous-variable quantum key distribution with Gaussian modulation—the theory of practical implementations", *Advanced Quantum Technologies*, vol. 1, no. 1, 2018.
- [3] *PETRUS to Showcase Groundbreaking "Mini EuroQCI" Quantum Key Distribution Demo at ECOC 2024 network, highlighting the future of secure communication*. <https://petrus-euroqci.eu/events/>, Accessed: 2025-04-30.
- [4] S. Yang, Z. Yan, H. Yang, *et al.*, "Information reconciliation of continuous-variables quantum key distribution: Principles, implementations and applications", *EPJ Quantum Technology*, vol. 10, no. 1, p. 40, 2023.
- [5] A. A. E. Hajomer, F. Kanitschar, N. Jain, *et al.*, "Experimental composable key distribution using discrete-modulated continuous variable quantum cryptography", *arXiv preprint arXiv:2410.13702*, 2024.
- [6] Y. Zhang, Z. Chen, S. Pirandola, *et al.*, "Long-distance continuous-variable quantum key distribution over 202.81 km of fiber", *Physical Review Letters*, vol. 125, no. 1, 2020, ISSN: 1079-7114.
- [7] A. A. Hajomer, A. Bomhals, C. Bruynsteen, *et al.*, "Chip-based 16 gbaud continuous-variable quantum key distribution", *arXiv preprint arXiv:2504.09308*, 2025.
- [8] H. Wang, Y. Li, T. Ye, *et al.*, "High-rate continuous-variable quantum key distribution over 100 km fiber with composable security", *arXiv preprint arXiv:2503.14843*, 2025.
- [9] M. Milicevic, C. Feng, L. M. Zhang, and P. G. Gulak, "Quasi-cyclic multi-edge LDPC codes for long-distance quantum cryptography", *npj Quantum Information*, vol. 4, no. 1, 2018.
- [10] K. Gümüş and L. Schmalen, "Low rate protograph-based LDPC codes for continuous variable quantum key distribution", *Proc. ISWCS 2021*, 2021.
- [11] C. Zhou, Y. Li, L. Ma, *et al.*, "A high-throughput and fpga-based LDPC decoder for continuous-variable quantum key distribution system", in *Quantum and Nonlinear Optics X*, SPIE, vol. 12775, 2023, pp. 62–66.
- [12] E. E. Cil and L. Schmalen, "Iteration-dependent scaled min-sum decoding for low-complexity key reconciliation in CV-QKD", in *Optical Fiber Communication Conference*, Optica Publishing Group, 2024, W4C–8.
- [13] Y. Chen, X.-Q. Jiang, G. Chen, P. Huang, E. Bai, and H. Hai, "Efficient fpga implementation of syndrome-assisted layered belief propagation decoder for CV-QKD systems", in *2024 9th International Conference on Communication, Image and Signal Processing (CCISP)*, IEEE, 2024, pp. 97–101.
- [14] F. Kienle and N. Wehn, "Low complexity stopping criterion for LDPC code decoders", in *2005 IEEE 61st Vehicular Technology Conference*, vol. 1, 2005, 606–609 Vol. 1.
- [15] T. A. Eriksson, R. S. Luís, K. Gümüş, *et al.*, "Digital self-coherent continuous variable quantum key distribution system", in *Optical Fiber Communication Conference*, Optica Publishing Group, 2020, T3D–5.
- [16] S. van der Heide, J. Frazão, A. Albores-Mejía, and C. Okonkwo, "Receiver noise stability calibration for CV-QKD", *Proc. OFC 2023*, 2023.